

Role of low-frequency vibrations on sound propagation in glasses at intermediate temperature

A. Criado, M. Jiménez-Ruiz, C. Cabrillo, and F. J. Bermejo

Consejo Superior de Investigaciones Científicas, Serrano 123, E-28006 Madrid, Spain

and Departamento de Física de la Materia Condensada, Universidad de Sevilla, P.O. Box 1065, E-41080 Sevilla, Spain

M. Grimsditch

Argonne National Laboratory, Argonne, Illinois 60439

H. E. Fischer

Institut Laue Langevin, Boîte Postale 156x, F-38042 Grenoble Cedex 9, France

S. M. Bennington and R. S. Eccleston

Rutherford Appleton Laboratory, Chilton Didcot, Oxon OX11 0QX, Great Britain

(Received 19 April 1999; revised manuscript received 3 January 2000)

We report measurements of the temperature dependence of the sound attenuation and the fractional change in sound velocity for the glass (G) and orientational-glass (OG) phases of polymorphic ethanol. Strikingly similar behaviors are found for both phases despite the OG's underlying crystal (bcc) lattice. Such similarity, which is also revealed in dielectric spectroscopy and inelastic neutron scattering measurements, suggests whole molecule small-angle librations as a common microscopic origin for a wide variety of "glassy" phenomena.

I. INTRODUCTION

The thermal,¹ elastic,² and dielectric³ behaviors of glasses largely differ from those of bulk crystalline solids at low and moderately high (tens of kelvins) temperature. In particular, some elastic properties such as sound velocity and attenuation in vitreous materials are known to exhibit remarkable anomalies if compared with those exhibited by the parent crystals. If expressed in terms of dimensionless quantities such as the fractional change in sound velocity with temperature $\delta v/v$ and the internal friction Q^{-1} , the former is found to increase with T below 1 K and strongly decrease at higher T ,⁴ whereas Q^{-1} shows an initial increase up to a few hundreds of millikelvins, then reaches a plateau of roughly constant Q_0^{-1} up to a few kelvins (a temperature referred usually as T^*), followed by an increase until a temperature dubbed T^{max} and finally, in some cases, a strong drop⁵ at even higher T has been reported. In addition, the measurements of sound attenuation in glasses are found to depend quite strongly on the measurement frequency, which is not the usual behavior for well-ordered crystals.

The above phenomena are explained on a phenomenological basis using concepts such as two-level systems⁶ (TLS), thermally activated relaxation,⁷ or some interpolation between the two such as the "soft-potential" model.⁸ The picture that emerges from most of these approaches portrays the dynamics of glasses below 5 K as dominated by coherent motion of TLS's weakly damped by relaxational and resonant interactions with elastic waves. The phase coherence of such motion is lost for $T > T^*$ mainly because of the onset of thermal motion. Finally, above T^* thermal occupation of excited levels of the interaction potential leads to a breakdown of the two-level approximation, and the dynamics becomes governed by thermally activated processes, which usually show an Arrhenius dependence of the relaxation rate.⁵

It has recently become clear that a more microscopic basis is required for a deeper understanding of the dynamics of glassy matter. This results from puzzling observations made on polycrystalline metallic solids,⁹ films or even bulk, deformed metallic solids¹⁰ that show that these materials behave as glasses and, even more, a comparison of such quantities carried out in metallic polycrystals in their normal and superconducting states⁹ suggests that the TLS's, if present in such materials, do not interact with the conduction electrons. In addition, other classes of partially ordered systems such as rotator-phase (or "plastic") crystals,¹¹ mixed crystals,¹² or even quasicrystals¹³ have shown dynamics that resemble that of amorphous matter. The ideal benchmark to clarify such apparently contradictory observations would then be constituted by a material that could be studied under controlled conditions of disorder. Such an endeavor has, however, not been carried out mainly because of the extreme difficulty in preparing glass samples having the same compositions as those employed for studies on polycrystals or rotator phases.

Here we consider a material that can easily be prepared in thermodynamically well-characterized phases such as the fully ordered, orientationally disordered, and amorphous phases of solid ethanol. A structural glass (G) is formed upon quenching the supercooled liquid below $T_g \sim 97$ K. The amorphous state can also be achieved using easily achievable cooling rates (≈ 6 K/min). Heating the glass above T_g yields a supercooled liquid that can be annealed to yield a rotator phase (RP, also referred in the literature as plastic or glassy crystal) phase. Once this is formed, cooling below $T_g^{OG} \sim 97$ K leads to a sluggish freezing of molecular rotations and an orientational glass (OG, or orientationally disordered crystal). The rotational freezing preserves the same crystal symmetry (an $Im\bar{3}m$ bcc lattice) of the RP, and from the structural point of view only a jump in the volume expansivity coefficient that amounts $\approx 4 \times 10^{-4} \text{ K}^{-1}$ accompanies

the transition.¹⁵ The latter is understood as a genuine glass-transition phenomenon of a purely dynamical origin.¹⁴ Previous studies have compared the structure¹⁵ and dynamics^{16,17} of the RP/OG and G phases, all showing very similar glassy behavior in their specific heats, vibrational frequency spectra, and dielectric spectroscopy to the stable fully ordered (monoclinic) crystal phase.

Our purpose here is thus to carry a comparative study on the dynamics of a material in its amorphous and orientationally disordered forms at meso- and microscopic scales. Since both the glass and OG solids have the same chemical composition as well as rather close densities, the differences in dynamic behavior, if any, will be entirely attributable to the presence in the OG of long-range periodicity. The present study will thus explore time and length scales in addition to those within the macroscopic realm as are those already examined using dielectric relaxation¹⁷ that have witnessed the dynamic proximity of the α and β relaxations of the glass (or supercooled liquid) and OG (or RP) phases.

II. LIGHT SCATTERING

We have measured the frequency and attenuation of hypersonic waves by Brillouin light scattering.¹⁸ The technique probes phonons with wavelengths comparable to that of light, the measured frequency shift ω_B is proportional to the sound velocity, and the width Γ of the Brillouin peak is related, through a convolution with the instrument function, to the attenuation. The sample was contained in a sealed copper cuvette attached to the cold finger and the temperature was controlled using a continuous flow cryostat.

The explored temperature interval was 5 K–120 K, which covers the range of both glassy phases (G and OG) as well as that of the RP crystal. As in previous experiments, all the phases were prepared *in situ* and carefully monitored. Below 5 K the low scattering intensity precluded the measurement. The temperature range investigated also covers the low-temperature anomaly [i.e., the excess in $C_p(T)/T^3$ specific heat with respect to the ordered crystal] and the region where the heat conductivity shows its ‘‘plateau.’’¹⁶ The measured spectra show Brillouin peaks arising from longitudinal elastic waves. Transverse sound modes are too weak to be observed. In addition, data already reported for fully hydrogenated glass and supercooled liquid samples at temperatures near the structural glass transition¹⁹ are included for comparison purposes.

Within the TLS framework, ω_B and Γ are related to the dispersive and dissipative parts of the susceptibility $\chi(\omega)$ by⁵

$$\frac{\delta\omega_B}{\omega_B} = \frac{\delta v}{v} = -\frac{A}{2}\chi'(\omega), \quad Q^{-1} = \frac{\Gamma}{\omega_B} = A\chi''(\omega),$$

$$A = \frac{g^2}{\rho v^2},$$

where A includes the ‘‘deformation potential’’ g (i.e., a measure of the coupling strength of TLS with elastic waves), mass density ρ , and sound velocity v . Our data for both glass and OG phases are shown in Fig. 1. Both graphs reveal the presence of two rather different regimes for both solids. Be-

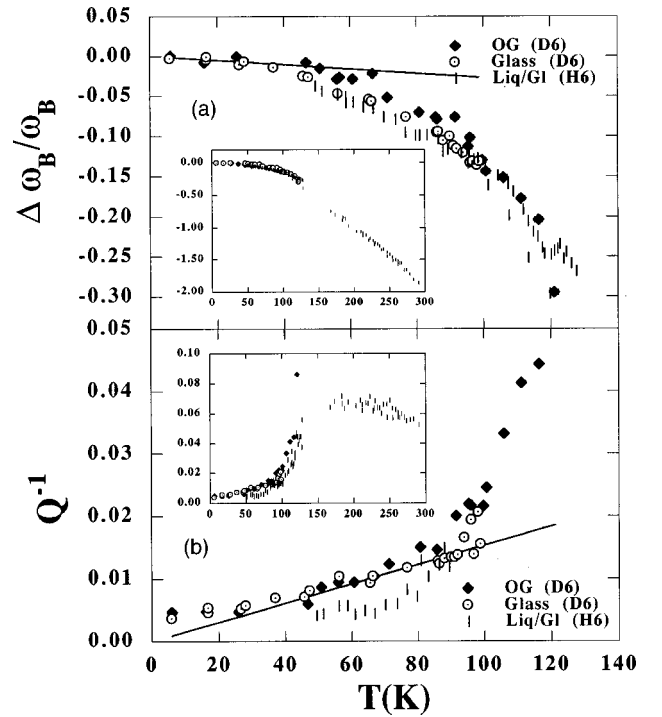


FIG. 1. (a) Fractional change of sound velocity with temperature for the glass (open symbols), OG/RP phases (filled symbols), and the data from Ref. 19 (vertical bars). The inset shows data covering the whole glass-transition region. The solid line shows an estimation using parameters given in the text. (b) Internal friction as a function of temperature (same symbols as above). The straight line depicts a prediction based on a thermal-activation model (Ref. 7).

low ≈ 30 K, the variation with T of $\delta v/v$ as well as Q^{-1} is rather mild, whereas a stronger T dependence is observed up to the glass transition (~ 100 K), and finally even more abrupt changes are seen in the supercooled-liquid or RP temperature range.

Our data for Q^{-1} at $T \approx 5$ K should be taken as an upper bound since they may be resolution limited. Taken at its face value the ≈ 5 K data are 2.7×10^{-3} (G) and 3.0×10^{-3} (OG). If we take these as representative of the ‘‘plateau’’ value of Q_0^{-1} , then they are above the average of those compiled by White and Pohl¹³ but compare with data for some metal films.¹⁰ If these values are used to make an estimate of the dimensionless constant⁵

$$C = \frac{2Q_0^{-1}}{\pi} = \frac{\bar{P}g^2}{\rho v^2}, \quad (1)$$

then one gets $C \approx 3.6 \times 10^{-3}$ and 5×10^{-3} . These are certainly larger than those reported for oxide glasses. However, our values come closer to those measured for electrolyte glasses as studied by Reichert *et al.*²¹ Those reported in Table 1 of Ref. 21 reach values up to $(9-9.6) \times 10^{-4}$ depending upon the salt content. In particular, the dependence of the constant C upon the content of salt (LiCl and ZnCl₂) given in percentage units follows a quasilinear law with a zero-salt limit of 1.34×10^{-3} . This is the value for C expected for an amorphous material chemically and structurally

not very dissimilar to ours such as amorphous water. In other words, our estimate for C comes close to others derived previously.

On the other hand, our values can also be understood on the basis of the linear correlations found by Hunklinger²⁰ and Reichert *et al.*²¹ between the quantities entering Eq. (1) and the glass transition temperature. In this respect, it is worth mentioning that both glassy ethanol and water show the highest densities of TLS states while the oxide glasses are found in the opposite extreme.

From ≈ 30 K up to T_g , Q^{-1} for both solids is well approximated by a linear temperature dependence with coefficients $1.68 \times 10^{-4} \text{ K}^{-1}$ (G) and $1.53 \times 10^{-4} \text{ K}^{-1}$ (OG). The implication is that data within this range pertain to a regime of thermally activated relaxation, which is governed by an Arrhenius relaxation rate. If such values are taken together with the previous estimate for C to make a guess for the zero point energy of the tunneling particle E_0 from Ref. 7 $Q^{-1} = \pi C k_B T / E_0$, one gets $E_0 = 18$ (19.9) K for G (OG), which is amazingly close to the 15 K derived for oxide glasses.⁵

Our data for Q^{-1} do not show maxima at T^{max} such as that found for oxide glasses by acoustic⁵ or Brillouin⁷ spectroscopies, probably because the appearance of both glass transitions at temperatures lower than that expected for T^{max} . From the inset of Fig. 1(a) one can, however, set the bounds $120 \text{ K} \leq T^{max} \leq 140 \text{ K}$.

III. RELATIONSHIP WITH MEASUREMENTS CARRIED OUT AT MACROSCOPIC SCALES

The β relaxation in both G and OG phases above ≈ 40 K has been recently studied by dielectric spectroscopy.¹⁷ The temperature dependence was describable in terms of an activation energy V_0 , a width of the energy-barrier distribution σ_0 , and the inverse of the attempt frequency τ_0 , having values of about 1000 K, 600 K, and 0.5×10^{-13} s, respectively. The parameters for both phases are the same within statistical precision. From data for τ_0 , as well as from the estimate of T^{max} given above, one obtains an upper bound for V_{max} , which is the upper limit of the distribution function of the barrier heights for states that fulfill the condition $\omega \tau = 1$, as⁷ $k_B T^{max} = -V_{max} / \ln(\omega \tau_0)$ with ω being the observation frequency. The result yields $V_{max} = 720$ K for a temperature of 130 K, in the midpoint of the interval given above. If we now consider how $\delta v/v$ is expected to behave in a thermally activated regime fulfilling $\omega \tau_0 \ll 1$, namely, $\delta v/v = C k_B T \ln(\omega \tau_0) / E_0$, we find that, using the parameters referred to above, the description becomes valid up to $T \approx 60$ K as Fig. 1 shows. The stronger decrease in $\delta v/v$ above this temperature is probably a signature of the increasing importance of thermal expansion effects not accounted for by the model.

Our previous study¹⁷ enabled the identification of thermally activated low-angle reorientations (librations), which are strongly coupled to the collective (phonon) modes, as the main microscopic entity giving rise to the dielectric signal of both G and OG.¹⁷ Moreover, such motions show a peaked density of states that accounts for the excess in the $C(T)/T^3$ specific heat plots at about 5–8 K as well as to the ‘‘plateau region’’ in thermal conductivity.¹⁶ From the closeness of the

thermal activation parameters at both macro- (dielectric) and mesoscopic (Brillouin) scales, we infer that mechanisms similar to those causing dielectric relaxation should be responsible for the observed behavior of $\delta v/v$ and Q^{-1} . Such motions should then be considered akin to those ‘‘additional harmonic excitations’’ comprising correlated motions of a few structural units in the well studied case of vitreous SiO_2 .

IV. DYNAMICS AT MICROSCOPIC SCALES

To explore the nature of the motions referred to above that have frequencies commensurate with maxima in $C(T)/T^3$, that is, $2 \text{ meV} \leq \omega \leq 4 \text{ meV}$, a number of measurements by neutron spectroscopy were carried out using the MARI spectrometer at the ISIS pulsed neutron source (Rutherford Appleton Laboratory, U.K.). The sample was fully deuterated ethanol, which allowed us to monitor continuously its state by inspection of the diffraction patterns, and was contained in a standard aluminum sample can.

The measurements were carried using incident energies of $E_i = 100 \text{ meV}$ and $E_i = 15 \text{ meV}$. This was done in order to cover a large kinematic region so that the dependence of the dynamic structure factor $S(Q, \omega)$ with wave vector can be safely explored and also to detect the possible existence of excitations occurring at finite frequency and constant wave vector.

In view of the strong anharmonic effects displayed in Fig. 1, the measurements were carried at relatively low temperatures (about 5 K) that are close to those where $C(T)/T^3$ also show their maxima.¹⁶ As an added bonus, carrying out the measurement at such temperatures diminishes the importance of multiexcitation contributions. All three solids were prepared *in situ* after an initial quench of the high-temperature liquid into the deep glass phase. The spectra corresponding to the amorphous solids were the ones first measured. The orientationally disordered crystals were prepared by raising the temperature 10 K above T_g and a subsequent annealing under such conditions. Formation of the RP crystal was well monitored by the appearance of a strong Bragg peak in the diffraction pattern measured using the elastic $I(Q, \omega = 0)$ channels (integrated over resolution width). Finally, the stable monoclinic phase was prepared by annealing at temperatures close to its melting $T_m = 159$ K for a few hours. The diffraction patterns of the three solids are shown as insets of Fig. 3. Data reduction and analysis followed standard routes. Because of the high transmission of our sample multiple-scattering contributions to the measured spectral patterns were estimated to be rather small. Finally, the multiphonon contributions were evaluated following the procedure described in Ref. 22 and subtracted from the bare intensity.

Figure 2 displays a representative set of spectra measured with $E_i = 15 \text{ meV}$, which enables one to compare directly the intensity patterns of the three solids. This allows us to see that there is no measurable difference in the spectra of the two glassy solids, while a substantially different behavior is followed by the ordered (monoclinic) crystal. The largest difference in intensities concern a range of frequencies that stretches up to frequencies commensurate with those where the monoclinic crystal shows its first intense phonon band ($\approx 6 \text{ meV}$). It concerns an easily visible ‘‘excess’’ of inelas-

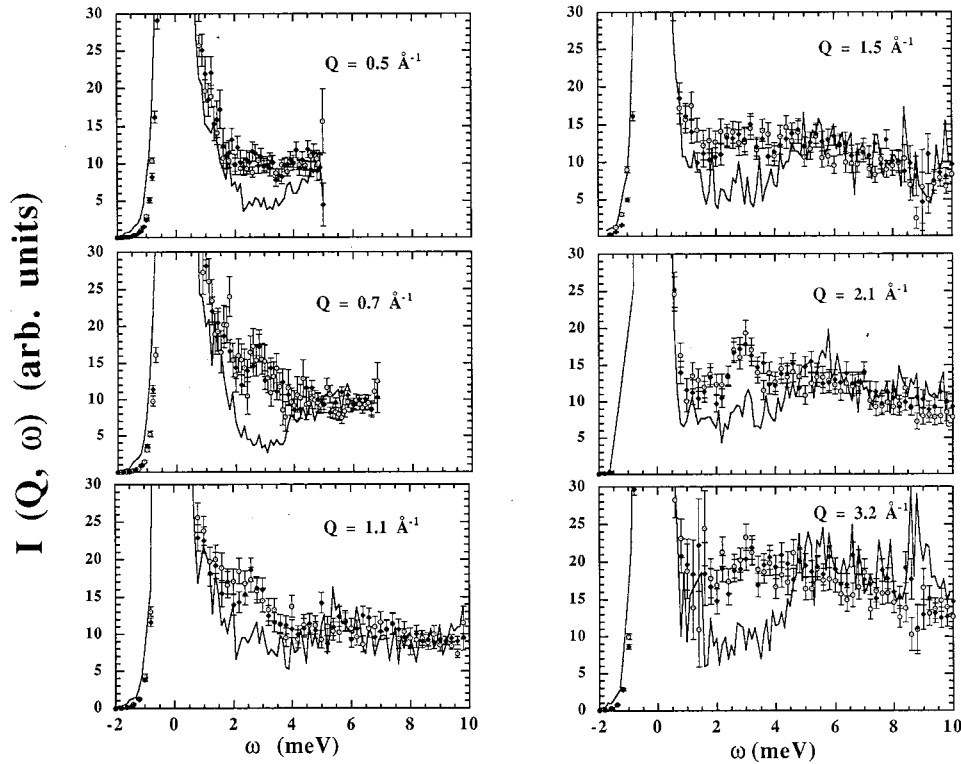


FIG. 2. Constant- Q spectra as measured using an incident energy $E_i = 15$ meV for values of the momentum transfer given in the insets. The solid line depicts the spectra of the monoclinic crystal, the open symbols show the spectra for the glass, and the filled symbols the spectra of the orientationally disordered crystal.

tic intensity of both glass and OG with respect to the ordered crystal, which reaches a maximum at frequencies within the range 2–3 meV. Such “excess modes” once averaged over momentum transfers will give rise to vibrational frequency distributions such as those reported in some of our previous studies.²³

With respect to the wave-vector dependence of the inelastic intensities shown in Fig. 2 the following qualifications should be taken into account. Below $Q \approx 0.5 \text{ \AA}^{-1}$ the inelastic intensities of the glassy solids show a rather structureless shape. That of the ordered crystal grows steeply from the tail of the elastic line and crosses those of the glassy solids at about 5 meV. A small maximum starts to develop at about 2.5 meV in the spectra of both glassy solids for $Q = 0.7 \text{ \AA}^{-1}$. From there to the largest explored wave vectors such a maximum appears as a dispersionless feature and can be identified with the “boson peak” found in studies employing incoherent-scattering samples.^{16,11} What seems worth exploring is the observation that while the center of such a peak does not show any clear dependence with wave vector, the amount of excess intensity shown by the two glasses with respect to the crystalline ground state shows some modulation with Q . For wave vectors corresponding to the first Brillouin zone of the ordered crystal (e.g., below 0.85 \AA^{-1}) the excess intensities are maximal. Such a difference gets almost suppressed when approaching the Brillouin zone boundary and reappears as one proceeds further.

Having measured $S(Q, \omega)$ for relatively large Q 's enables us to consider in some detail the quantity $S(Q, \omega = \text{const})$, that is, the wave-vector dependence of the inelastic intensity for the range of frequencies where the excess modes commented on above is maximal. Such quantities are, in fact, inelastic structure factors, giving information about the vector displacements of the atoms taking place in such motions. A model-free assessment of the nature of motions being

sampled is provided by comparison of the phases of oscillations in $S(Q, \omega = \text{const})$ with those shown by the static $S(Q)$ or elastic $S(Q, \omega = 0)$ structure factors. Purely translational motions (i.e., long-wavelength acoustic phonons) leave all distances unaltered and therefore $S(Q, \omega = \text{const})$ should show oscillations in phase with those of $S(Q)$ or $S(Q, \omega = 0)$.

Cuts of $S(Q, \omega = \text{const})$ for $2.5 \text{ meV} \leq \omega \leq 3.5 \text{ meV}$, an interval free from any substantial contamination by the elastic line, are shown in Fig. 3. Both glassy solids (G and OG) show a strikingly similar intensity pattern, with a shoulder at about 3 \AA^{-1} , a broad maximum at 7 \AA^{-1} , and a minimum at about 11.2 \AA^{-1} . Only a small peak is seen for G and OG at Q values corresponding to the main peak in the diffraction pattern $Q_p \approx 1.7 \text{ \AA}^{-1}$. In contrast, sharp peaks at 1.7 \AA^{-1} and 2.5 \AA^{-1} identify the presence of propagating excitations in the spectrum for the monoclinic crystal, a feature also reproduced from a crystal lattice dynamics calculation. This shows that even at these relatively low frequencies, most of the intensity in spectra of the glassy solids arises from motions not involving in-phase displacements of the molecular centers of mass (COM). In other words, most of the intensity at frequencies comparable to that of the “boson peak” seem to arise from motions that should have a molecular reorientational component as dominant, as explained.

Now we take advantage of the presence within the OG phase of a crystal bcc cell as well as the availability of the absolute frequency scale provided by the monoclinic crystal. This enables the separation of purely translational and rotational motions since the molecular centers of mass sit at the nodes of the bcc lattice. We have carried out a number of computer simulations for such a model of the OG crystal. Our point of departure was to assume that relative molecular orientations all have the same statistical weight, a fact grounded on previous results.¹⁵ A random sampling strategy

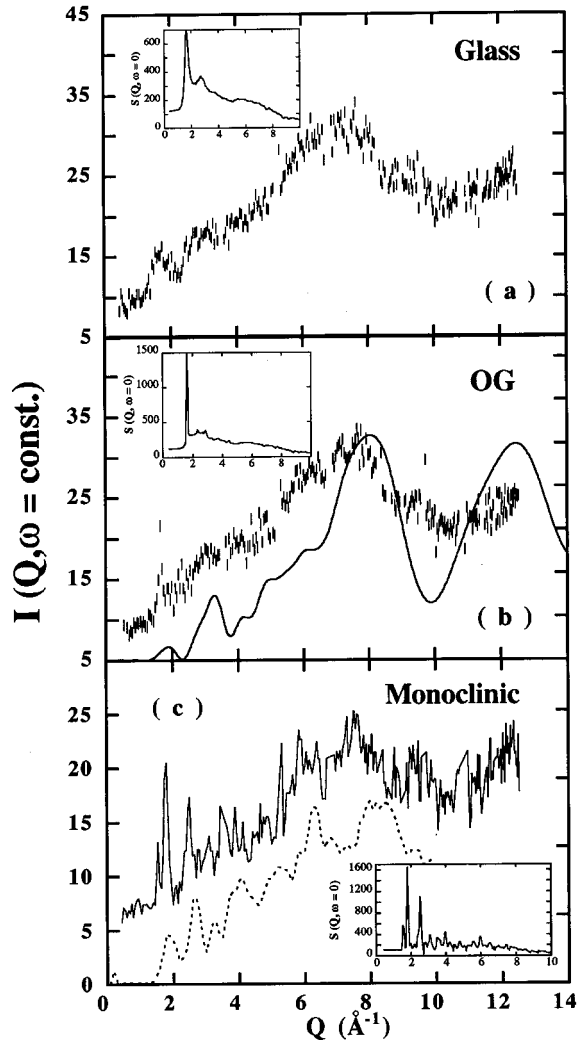


FIG. 3. Neutron spectroscopy data at constant frequency $I(Q, 2.5 \text{ meV} < \omega < 3.5 \text{ meV})$ for the glass, OG, and monoclinic crystal phases at $T = 5 \text{ K}$ [frames (a)–(c), respectively]. The solid line shown in frame (b) corresponds to the calculation made for the bcc crystal on the basis of Eq. (2). The dashed line shown in frame (c) depicts the result from a harmonic lattice dynamics calculation for the monoclinic powder (see Ref. 16). Insets display the elastic $I(Q, \omega = 0)$ data.

was devised to generate the initial molecular orientations as well as the small librational displacements. Molecular COM motions were simulated by displacing the molecules along the Cartesian displacement coordinates of the bcc lattice. A further average was then taken over the different displacement modes and the final atomic displacement vectors \mathbf{u}_i were calculated. The calculated inelastic structure factor $I(Q, \omega = \text{const})$ was finally evaluated from the one-phonon partial structure factors $F_{ij}(Q)$,

$$I(Q, \omega = \text{const}) \propto \sum_i \sum_{j \neq i} F_{ij}(Q) G(\omega), \quad (2)$$

$$F_{ij}(Q)/Q^2 = \frac{1}{\sqrt{M_i M_j}} \left[\frac{1}{3} (\mathbf{u}_i \cdot \mathbf{u}_j) j_0(Q d_{ij}) + \left(\frac{1}{3} (\mathbf{u}_i \cdot \mathbf{u}_j) - \frac{1}{d_{ij}^2} (\mathbf{d}_{ij} \cdot \mathbf{u}_j) \right) j_2(Q d_{ij}) \right], \quad (3)$$

where M_i are atomic masses, \mathbf{u} are vector displacements, \mathbf{d}_{ij} are vectors joining two atoms, $G(\omega)$ are spectral functions (combination of Bose factors and δ peaks), and $j_x(\cdot)$ are spherical Bessel functions.

The calculated curve is compared with experiment after addition of a self-scattering component²⁴ and is shown in Fig. 3. The result shows that purely translational motions contribute to the observed intensity at such frequencies with only a small feature at $Q = Q_p$. In contrast, reorientational excursions with an average angle of about 0.3° account for the shape of $I(Q, \omega = \text{const})$.

Because of the very close similarity of the experimental inelastic structure factor for the OG and the fully disordered solid, one expects that the results for the former, here considered as a reference “glass,” should also be of relevance for the latter. In other words, they serve to quantify the contribution to $I(Q, \omega)$, on \AA and picosecond scales, coming from purely acoustic motions certainly involving the displacements of molecular COM’s, versus those arising from additional (librational) excitations. From the very small weight of the peak at $Q = Q_p$ we infer that a high-frequency cutoff for the existence of well-defined soundlike excitations should not be far beyond $\omega_{co} \leq 3 \text{ meV}$, a frequency that becomes comparable to that of the “boson peak.”

V. CONCLUSIONS

The findings reported here are of relevance to our understanding of glassy dynamics since they enable a coherent description of the mechanisms driving the dynamics of disordered matter at widely different spatiotemporal scales as explored by dielectric (macro-), Brillouin (meso-), and neutron (microscopic) spectroscopies. A number of characteristic phenomena can be understood as resulting from the interaction of long-wavelength acoustic waves with small-amplitude molecular librations. The latter are known to give rise to the peak in $C(T)/T^3$, constitute an efficient mechanism for sound attenuation via relaxational and resonant scattering mechanisms, and explain the concomitant reduction in sound velocity with temperature. The present results also suggests a set of weakly damped (TLS) librators resonantly interacting with sound waves as the most feasible entities giving rise to the linear term in the specific heat below 2 K found for the bcc crystal and glass.¹⁶

ACKNOWLEDGMENTS

We acknowledge support from DGICYT (Spain) Grant No. PB95-0075-C03-01 and U. S. Department of Energy, Basic Energy Sciences–Materials Sciences under Contract No. W-31-109-ENG-38.

- ¹R. C. Zeller and R. O. Pohl, Phys. Rev. B **4**, 2029 (1971).
- ²K. A. Topp and D. G. Cahill, Z. Phys. B: Condens. Matter **101**, 235 (1996).
- ³S. Hunklinger *et al.*, in *Amorphous Solids: Low Temperature Properties*, edited by W. A. Phillips (Springer, Berlin, 1981), p. 81.
- ⁴S. Rau, C. Enss, S. Hunklinger, P. Neu, and A. Würger, Phys. Rev. B **52**, 7179 (1995).
- ⁵A. Würger, *From Coherent Tunneling to Relaxation* (Springer, Berlin, 1997), p. 116.
- ⁶J. Jäckle, Z. Phys. **257**, 212 (1972); J. Black and P. Fulde, Phys. Rev. Lett. **43**, 453 (1979).
- ⁷D. Tielbörger, R. Merz, R. Ehrenfels, and S. Hunklinger, Phys. Rev. B **45**, 2750 (1992).
- ⁸U. Buchenau, Y. M. Galperin, V. L. Gurevich, D. A. Parshin, M. A. Ramos, and H. R. Schober, Phys. Rev. B **46**, 2798 (1992).
- ⁹R. König, P. Esquinazi, and B. Neppert, Phys. Rev. B **51**, 11 424 (1995); E. Gaganidze, P. Esquinazi, and R. König, Europhys. Lett. **31**, 13 (1995).
- ¹⁰X. Liu, E. Thompson, B. E. White, Jr., and R. O. Pohl, Phys. Rev. B **59**, 11 767 (1999).
- ¹¹M. A. Ramos, S. Vieira, F. J. Bermejo, J. Dawidowski, H. E. Fischer, H. Schober, M. A. González, C. K. Loong, and D. L. Price, Phys. Rev. Lett. **78**, 82 (1997).
- ¹²J. P. Sethna, E. R. Grannan, and M. Randeria, Physica B **169**, 316 (1991), and references therein.
- ¹³B. E. White and R. O. Pohl, Z. Phys. B: Condens. Matter **100**, 401 (1996).
- ¹⁴M. Jiménez-Ruiz, A. Criado, F. J. Bermejo, G. J. Cuello, F. R. Trouw, R. Fernandez-Perea, H. Lowen, C. Cabrillo, and H. E. Fischer, Phys. Rev. Lett. **83**, 2757 (1999).
- ¹⁵R. Fayos, F. J. Bermejo, J. Dawidowski, H. E. Fischer, and M. A. González, Phys. Rev. Lett. **77**, 3823 (1996); F. J. Bermejo, A. Criado, R. Fayos, R. Fernandez-Perea, H. E. Fischer, E. Suard, A. Gueylyah, and J. Zñiga, Phys. Rev. B **56**, 11 536 (1997).
- ¹⁶C. Talón, M. A. Ramos, S. Vieira, G. J. Cuello, F. J. Bermejo, A. Criado, M. L. Senent, S. M. Bennington, H. E. Fischer, and H. Schober, Phys. Rev. B **58**, 745 (1998); S. Vieira, M. A. Ramos, Q. W. Zou, and C. Talón, Phase Transit. **64**, 87 (1997).
- ¹⁷M. A. Miller, M. Jiménez-Ruiz, F. J. Bermejo, and Norman O. Birge, Phys. Rev. B **57**, R13 977 (1998); M. Jiménez-Ruiz, M. A. González, F. J. Bermejo, M. A. Miller, N. O. Birge, I. Lendoya, and A. Alegria, *ibid.* **59**, 9155 (1999); M. A. González *et al.*, Phys. Rev. E (to be published).
- ¹⁸J. Sandercock, in *Light Scattering in Solids III*, Topics in Applied Physics Vol. 51 (Springer, New York, 1979).
- ¹⁹A. Srinivasan, F. J. Bermejo, and A. Bernabe, Mol. Phys. **87**, 1439 (1996).
- ²⁰S. Hunklinger, in *Heidelberg Colloquium on Glassy Dynamics*, edited by J. L. van Hemmen *et al.* (Springer, Berlin, 1987), p. 110. Such correlations would yield about 0.05 eV for g and $\approx 10^{34}$ erg $^{-1}$ cm $^{-3}$ for \bar{P} , which together with $v=2.6 \times 10^5$ cm s $^{-1}$ and $\rho=0.98$ g cm $^{-3}$ leads to $C=9.7 \times 10^{-4}$.
- ²¹U. Reichert, M. Schmidt, and S. Hunklinger, Solid State Commun. **57**, 315 (1986). The article includes a data point for amorphous water in Fig. 3. An alternative view on the meaning of linear correlations between the TLS parameters and the glass-transition temperature is given by J. F. Berret and M. Meissner, Z. Phys. B: Condens. Matter **70**, 65 (1988).
- ²²J. Dawidowski, F. J. Bermejo, and J. R. Granada, Phys. Rev. B **58**, 706 (1998).
- ²³H. E. Fischer, F. J. Bermejo, G. J. Cuello, M. T. Fernández-Díaz, J. Dawidowski, M. A. González, H. Schober, and M. Jiménez-Ruiz, Phys. Rev. Lett. **82**, 1193 (1999).
- ²⁴A. C. Hannon, M. Arai, and R. G. Delaplane, Nucl. Instrum. Methods Phys. Res. A **354**, 96 (1995).